Title

Can Fluxionality of Subnanometer Cluster Catalysts Solely Cause Non-Arrhenius Behavior in Catalysis?

Journal

The Journal of Physical Chemistry C, 124(36)

ISSN

1932-7447

Authors

Zandkarimi, Borna
Alexandrova, Anastassia N

Publication Date

2020-09-10

DOI

10.1021/acs.jpcc.0c04136

Peer reviewed

Can Fluxionality of Subnanometer Cluster Catalysts Solely Cause Non-Arrhenius Behavior in Catalysis?

Borna Zandkarimi[a] *and Anastassia N. Alexandrova*[a,b]*

[a]Department of Chemistry and Biochemistry, University of California, Los Angeles, Los Angeles, CA 90095

[b]California NanoSystems Institute, 570 Westwood Plaza, Los Angeles, CA 90095

*Corresponding Author: Anastassia N. Alexandrova, +1 (310) 825-3769, ana@chem.ucla.edu

Abstract

Supported sub-nano clusters are intriguing catalysis, which can present an ensemble of many distinct and easily interconverting geometric states to the reactive medium in catalytic conditions. Each of these states can contribute to catalysis with a unique reaction rate. We argue that such sub-nano cluster catalysts can in principle show a non-Arrhenius behavior, thanks to their structural fluxionality. However, it is unlikely to see this in practice due to the stringent requirements on the heights of the reaction barriers involved. Furthermore, we demonstrate that the ensemble average rate constant which was previously proposed to be used for the ensemble of fluxional clusters to describe the catalytic properties of the system is the same as Tolman's formula proposed in 1920. Note that in this study we only isolate the dynamicity of clusters as one factor that can affect the kinetics of catalysis. We also propose that calculating $\frac{1}{k_B}(\langle E_{TS}\rangle - \langle E_R\rangle)$ as a function of T can be used as a good indicator of a possible non-Arrhenius behavior.

1. Introduction

The impressive empirical relationship between the rate constant of a reaction and its activation energy, which was proposed by Svante Arrhenius[1] in 1889, and is still widely used in catalysis, can be written as

$$k(T) = Ae^{-\frac{E_a}{k_B T}} \quad (1)$$

, where A is the pre-exponential factor, E_a is the activation energy, and k_B is the Boltzmann constant.[2–4] Recently, it has been shown that, for dynamic catalytic interfaces, metastable structures of the catalyst rather than the global minimum can play an important role in defining the thermodynamic and the kinetic properties of the interfaces.[5–7] Perhaps the most dramatic example of such an interface are supported nano- and sub-nano clusters. The potential energy surface of metal clusters can have several stable structures (local minima) with different energies. The difference between the energies originates from their differences in geometries and electronic structures (chemical bonding, spin states). Since different isomers have different structure, spin state, and energy, their frontier molecular orbitals look differently and have different energetics. This affects their interaction with the reagents, and the resultant reaction pathways and barriers. An ensemble-average approach was introduced to capture the contribution of important low-lying isomers to the properties of such systems.[8–10] For the kinetics, one can define the ensemble average rate constant based on the all thermally-accessible isomers populated at reaction temperature as[11,12]

$$k_{ens} = \sum_{i}^{n} P_i A_i e^{\frac{-E_{a,i}}{k_B T}} \quad (2)$$

, where P_i is the Boltzmann population of isomer i at temperature T, which can be written as

$$P_i \approx \frac{e^{\frac{-E_i}{k_B T}}}{\sum_i e^{\frac{-E_i}{k_B T}}} \quad (3)$$

, assuming that only the electronic energy contribution is important, and ignoring the degeneracy. In general, if we neglect the temperature-dependence of the pre-exponential factor, the $\ln(k)$ vs. $1/T$ plot should be linear, and the slope of this plot is equal to $-E_a/k_B$. For an ensemble of fluxional clusters, we can use k_{ens} defined in equation (2) and calculate the slope of $\ln(k_{ens})$ vs. $1/T$ plot as

$$slope = \frac{d(lnk_{ens})}{d\left(\frac{1}{T}\right)} = \frac{1}{k_B}\left(\frac{\sum_i^n E_i e^{\frac{-E_i}{k_B T}}}{\sum_i^n e^{\frac{-E_i}{k_B T}}} - \frac{\sum_i^n (E_i + E_{a,i}) e^{\frac{-(E_i+E_{a,i})}{k_B T}}}{\sum_i^n e^{\frac{-(E_i+E_{a,i})}{k_B T}}}\right) \quad (4)$$

(See Appendix A for detailed derivation). As can be seen from equation (4), the first term in parentheses is nothing but the ensemble average energy of the reactants $\langle E_R \rangle$ and the second term can be interpreted as the ensemble average energy of the transition states $\langle E_{TS} \rangle$. Hence, we can write the activation energy corresponding to an ensemble of fluxional clusters as

$$\langle E_a \rangle = \langle E_{TS} \rangle - \langle E_R \rangle \quad (5)$$

Equation (5) shows that the activation energy of an ensemble of fluxional clusters can be written as the difference between the ensemble average energies of the transition states and the reactants corresponding to all thermally-accessible isomers at the reaction temperature. This finding is, in fact, similar to what Tolman[13] proposed in 1920 based on a statistical mechanic approach. He suggested that the activation energy of a reaction can be defined as the difference in the average energy of reacting species minus the average energy of reactant species. Moreover, Truhlar,[14] using reactive cross sections in collision theory, further expanded Tolman's interpretation of the activation energy. Recently, Piskulich et al.[15] wrote an informative feature article on the interpretation of activation energies for dynamical processes, and the new approaches that use the fluctuation theory to determine the activation energy for an arbitrary dynamical time scale at a single temperature. Here, based on what we proposed in equations (2) – (5), we try to investigate whether fluxional catalytic clusters are able to exhibit a non-Arrhenius behavior solely due to their fluxionality. First, we investigate some hypothetical ensembles of clusters each characterized by a certain barrier of the catalyzed reaction, and then we discuss whether or not the effect is physically feasible in an actual catalytic system. Here we should emphasize that the effect of the adsorbate coverage, which can influence both the number and types of sites available at a heterogeneous surface, on the kinetics of the reaction has been studied before using ab intio modeling;[16] it is not the main focus of this study. Moreover, in the original Arrhenius paper,[1] he proposed his reaction rate model based on the inversion of cane sugar reaction by acids and never took into account the effect of coverage. In general, it is more informative to isolate each parameter (fluxionality in this case) and examine its isolated influence on our models.

In each theoretical ensemble case study, we set the relative energy of each isomer E_i, and its corresponding activation energy $E_{a,i}$, in order to calculate k_{ens}. Then for each case study we calculate R^2 corresponding to the $\ln(k_{ens})$ vs. $1/T$ plot in the range of 300 – 1000 K as a measure of linearity of the plot to determine whether the ensemble shows a non-Arrhenius behavior or not. Note that it has been shown that hundreds of isomers can be found especially for gas phase clusters by exploring the PES;[5,6,8,17] however, that does not mean that all of these structures contribute to the catalysis. Based on the Boltzmann population, only isomers which are within ~0.4 eV relative to the global minimum can have non-negligible populations at reaction temperatures (~ 700 K), while hirer-energy isomers remain unpopulated and thus, irrelevant to the catalysis. As a result, the ensemble energetics in this study are chosen such that they resemble realistic catalytic systems.[5,9,11,18] Furthermore, we assume that the observed activation energy, which is an ensemble average over the activations energies of all thermally-accessible isomers, rather than activation energy for each isomer will change as a function of temperature due to the change in the Boltzmann populations. Also, we assume that the pre-exponential factor is similar for different isomers of the same cluster (so no change as a function of T), while the activation energies are different. Since these isomers have different energies and stabilities, we believe it is a fair assumption to make. Since these isomers have different energies and stabilities, we believe it is a fair assumption to make.

2. Results and Discussion

In the first case study, we choose an ensemble of two isomers with the relative energies of $E_1 = 0$ and $E_2 = 0.05$ eV, which is not atypical in cluster catalysts. Then, we explore different combinations of $E_{a,1}$ and $E_{a,2}$ in the reasonable range of 0 – 2 eV with the step size of 0.01 eV, resulting in 40,000 different combinations. Figure 1a shows the whole search space, and Figure 1b shows the most significant part of the search space (low R^2), which constitutes of a very small region of the overall search space. As can be seen, based on the R^2 value obtained for all different combinations of $E_{a,1}$ and $E_{a,2}$, the majority of search space shows a clear Arrhenius behavior of the ensemble. There is only a very small region in which R^2 significantly deviates from 1.0, and that requires a very small $E_{a,1}$. In fact, for the ensemble of two isomers to show a non-Arrhenius behavior the activation energy corresponding to the global minimum ($E_{a,1}$) should be less than ~

0.025 eV. This small activation barrier makes the ensemble unlikely to exist (and show its non-Arrhenius behavior) in practice. It is also possible that the very small barrier may be indicative of a chemically unstable catalyst isomer 1. For example, such a cluster could strongly and irreversibly bind the products of the reaction step. Note that other possible relative energies in the ensemble have also been explored (summarized in Figure S1). It is clear from Figure S1 that the non-Arrhenius region still constitutes a small fraction of the overall search space. However, the larger the difference between E_1 and E_2, the smaller the region corresponding to the non-Arrhenius behavior. This is not unexpected since in that case the ensemble will become more and more dominated by the single global minimum structure.

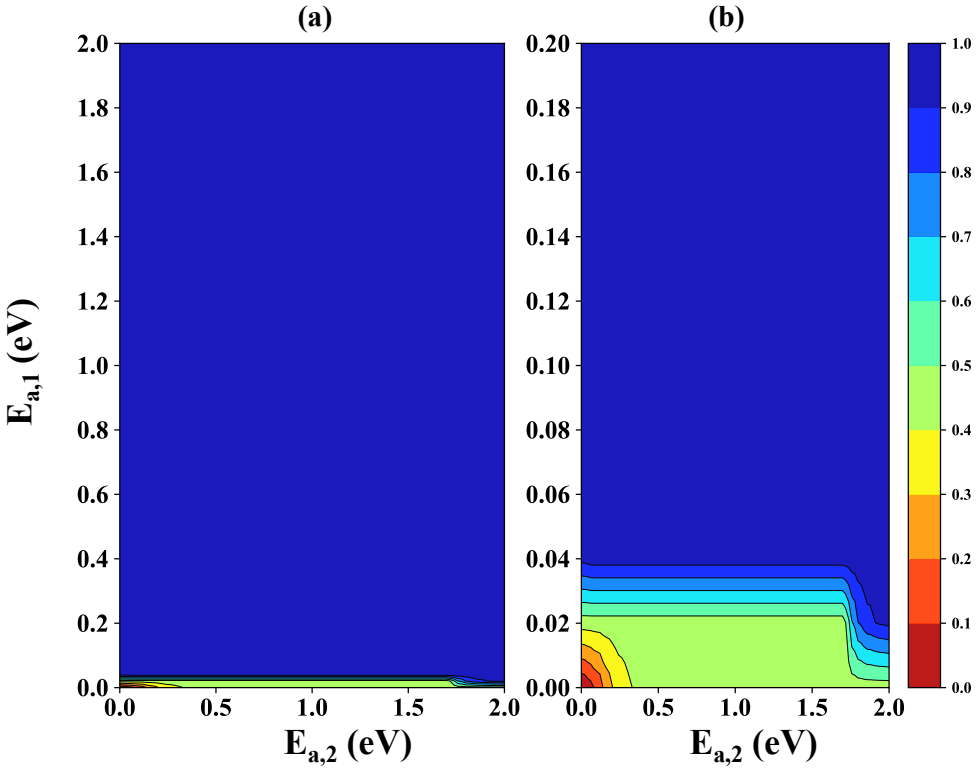

Figure 1. (a) R^2 value obtained from 40,000 different combinations of $E_{a,1}$ and $E_{a,2}$ in the range of 0 – 2 eV for the ensemble of two isomers with relative energies $E_1 = 0$ and $E_2 = 0.05$ eV. (b) The region with low R^2 values ($E_{a,1} < 0.2$ eV) is zoomed on. The temperature range in which R^2 is calculated is 300 – 1000 K.

In the next example we look at a more realistic catalytic system: an ensemble of 5 catalyst isomers with the relative energies of $E_1 = 0$, $E_2 = 0.01$, $E_3 = 0.10$, $E_4 = 0.15$, and $E_5 = 0.20$ eV. The energy distribution was chosen such that the included local minima get populated enough to affect the rate proportionally to their Boltzmann populations. Note that the search space of activation energies grows exponentially with the number of isomers; therefore, based on the results obtained for the ensemble of 2 isomers we change the step size from 0.01 eV to 0.1 eV for the activation energies between 0.1 – 2.0 eV (the less interesting region) but keep 0.01 eV as the step size for the activation energies between 0 – 0.1 eV (the more interesting region). This approach ensures that we still explore the important part of the search space but at the same time it keeps the computational cost at a reasonable level. All R^2 along with their corresponding $E_{a,i}$ values can be found in the SI. Some of the $E_{a,i}$ combinations with more realistic barriers along with their corresponding R^2 are summarized in Table 1.

Table 1. R^2 corresponding to $\ln(k_{ens})$ vs. $1/T$ plot of an ensemble of 5 isomers with the energy distribution of $E_1 = 0$, $E_2 = 0.01$, $E_3 = 0.10$, $E_4 = 0.15$, and $E_5 = 0.20$ eV obtained for different combinations of activation energies. The temperature range in which R^2 is calculated is 300 – 1000 K.

Ensemble	$E_{a,1}$ (eV)	$E_{a,2}$ (eV)	$E_{a,3}$ (eV)	$E_{a,4}$ (eV)	$E_{a,5}$ (eV)	R^2 ($\ln k_{ens}$ vs. 1/T)
1	0.90	0.01	0.80	0.60	0.70	0.7298
2	1.90	0.01	1.80	1.60	1.70	0.7286
3	2.00	0.01	1.90	1.80	1.90	0.7290
4	0.60	0.01	1.80	0.50	0.20	0.7853
5	1.90	0.02	1.80	1.60	1.70	0.9468
6	0.01	0.20	1.80	0.20	1.80	2×10^{-5}
7	0.01	1.90	1.00	0.70	1.60	0.4683
8	0.01	0.01	0.08	1.70	0.30	0.6433
9	0.02	0.40	1.40	0.30	0.80	0.7987

It is clear from Table 1 that there are some ensembles with low R^2 in which $E_{a,2}$ rather than $E_{a,1}$ is the smallest barrier. In these cases, the reaction kinetics is dominated by the second isomer rather than the global minimum. On the other hand, there are many cases where the global minimum isomer has the smallest barrier and still the ensemble shows a non-Arrhenius behavior. However, in all cases that show a non-Arrhenius behavior, there should be at least one barrier lower than 0.02 eV, and no cases were found where $R^2 < 0.8$ and all $E_{a,i} > 0.02$ eV. Note that the energy of

the isomer 2 in the ensemble is very close to the energy of the global minimum, which is something that can happen in practice. This can affect the ensemble rate constant if the barriers corresponding to these isomers are significantly different which is apparent from Table 1. Nevertheless, there are some cases in which $E_{a,1} = E_{a,2}$ and the ensemble still shows a non-Arrhenius behavior (see, for example, ensemble 8 in Table 1).

Figure 2 shows how the ensemble behaves as the barrier becomes larger ($E_{a,2}$ changes from 0 to 0.05 eV), while other parameters of the ensemble are kept constant. We choose ensemble 2 from Table 1 as an example in this case. One can see that for $E_{a,2} < 0.02$ eV the plot is clearly non-Arrhenius; however, once $E_{a,2}$ becomes larger than that the ensemble shows the Arrhenius behavior. Furthermore, the plots in Figure 2 are similar to the ones that can be found in the Marcus inverted region.[19–25]

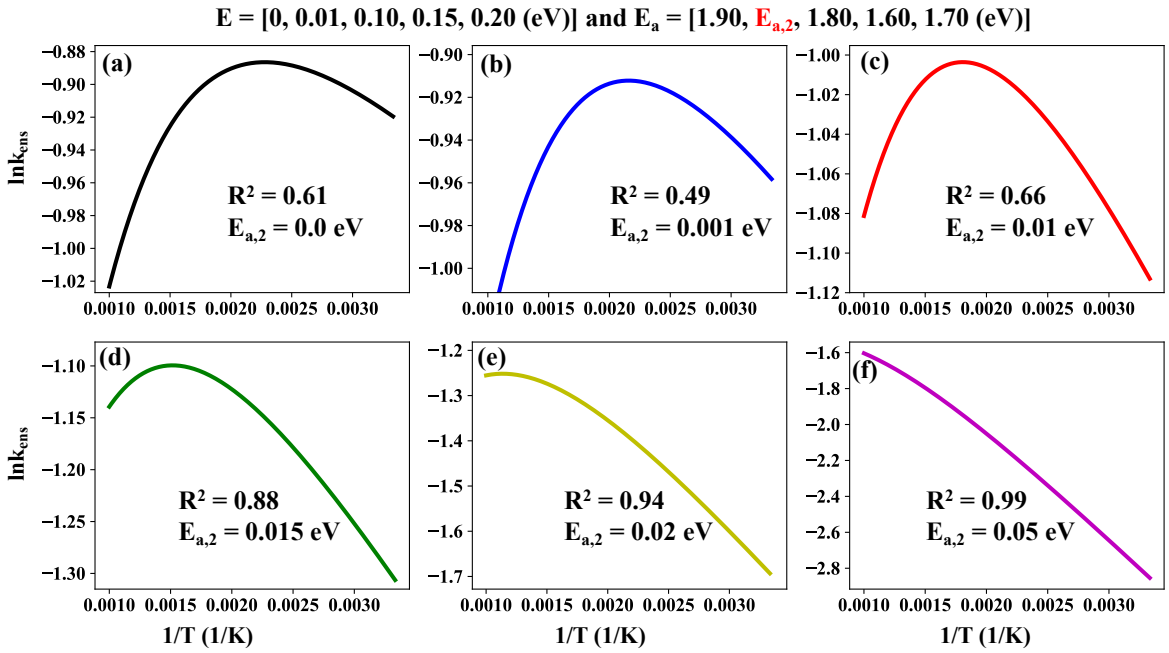

Figure 2. (a) – (f) Arrhenius plots of the ensemble of 5 isomers with relative energies of E = [0, 0.01, 0.1, 0.15, 0.2 eV] and activations energies of E_a = [1.90, $E_{a,2}$, 1.80, 1.60, 1.70 eV] in the temperature range of 300 – 1000 K as a function of $E_{a,2}$. Note that for $E_{a,2} > 0.05$ eV the plot becomes completely linear. ($R^2 > 0.99$)

In addition, we investigate how the energy distribution in the ensemble can affect the R^2. In this case, we keep the activation energies constant and instead change the relative energies of the isomers in the ensemble. As an example, we choose ensemble 2 from Table 1 which was found in the previous search and change the relative energies in the ensemble. Note that, once the relative energies become large, they no longer contribute to the ensemble; therefore, the energies should be chosen such that each isomer still can contribute to the ensemble rate constant. The obtained results are summarized in Table 2. Here, once the energy of second isomer relative to the global minimum reaches 0.05 eV, the correlation value becomes ~ 0.98 and the plot becomes linear.

Table 2. R^2 of $\ln k_{ens}$ vs. $1/T$ plot of an ensemble of 5 isomers with the activation energies of $E_{a,1}$ = 1.90, $E_{a,2}$ = 0.01, $E_{a,3}$ = 1.80, $E_{a,4}$ = 1.60, and $E_{a,5}$ = 1.70 eV obtained for different combinations of activation energies. The temperature range in which R^2 is calculated is 300 – 1000 K.

E_1 (eV)	E_2 (eV)	E_3 (eV)	E_4 (eV)	E_5 (eV)	R^2 ($\ln k_{ens}$ vs. 1/T)
0	0.001	0.01	0.10	0.15	0.5585
0	0.01	0.10	0.15	0.20	0.7286
0	0.02	0.10	0.15	0.20	0.9024
0	0.05	0.10	0.15	0.20	0.9775

Furthermore, as can be seen from Figure 2, there is a maximum value for the reaction rate constant for the ensemble of 5 isomers. According to equation (5), the slope of the $\ln(k_{ens})$ vs. $1/T$ plot is $\frac{-1}{k_B}(\langle E_{TS}\rangle - \langle E_R\rangle)$. At the maximum of the plot the slope is zero; hence, to test the validity of equation (5) one can calculate $\frac{-1}{k_B}(\langle E_{TS}\rangle - \langle E_R\rangle)$ for the ensemble of interest, find the temperature at which the slope is zero, and compare it to the temperature that the plot itself shows at maximum. This shows that, for an ensemble, calculating $\frac{-1}{k_B}(\langle E_{TS}\rangle - \langle E_R\rangle)$ as a function of T is a good indicator whether the catalyst would show a non-Arrhenius behavior. To test it, we calculate $\frac{-1}{k_B}(\langle E_{TS}\rangle - \langle E_R\rangle)$ as a function of T for all cases shown in Figure 2 (see Figure 3). Based on Figure 3, the temperatures at which the slope becomes zero for $E_{a,2}$ = 0, 0.001, 0.01, 0.15, 0.02, and 0.05 eV are 439, 463, 660, 767, 880, and 2094 K respectively. This is in full agreement with Figure 2. Note that, for $E_{a,2}$ = 0.05 eV, we do not see the peak in the range of 300 – 1000 K. The change in

slope sign is apparent for the cases where $E_{a,2}$ < 0.02 eV in the temperature range of 300 – 1000 K, and that results in a non-Arrhenius behavior.

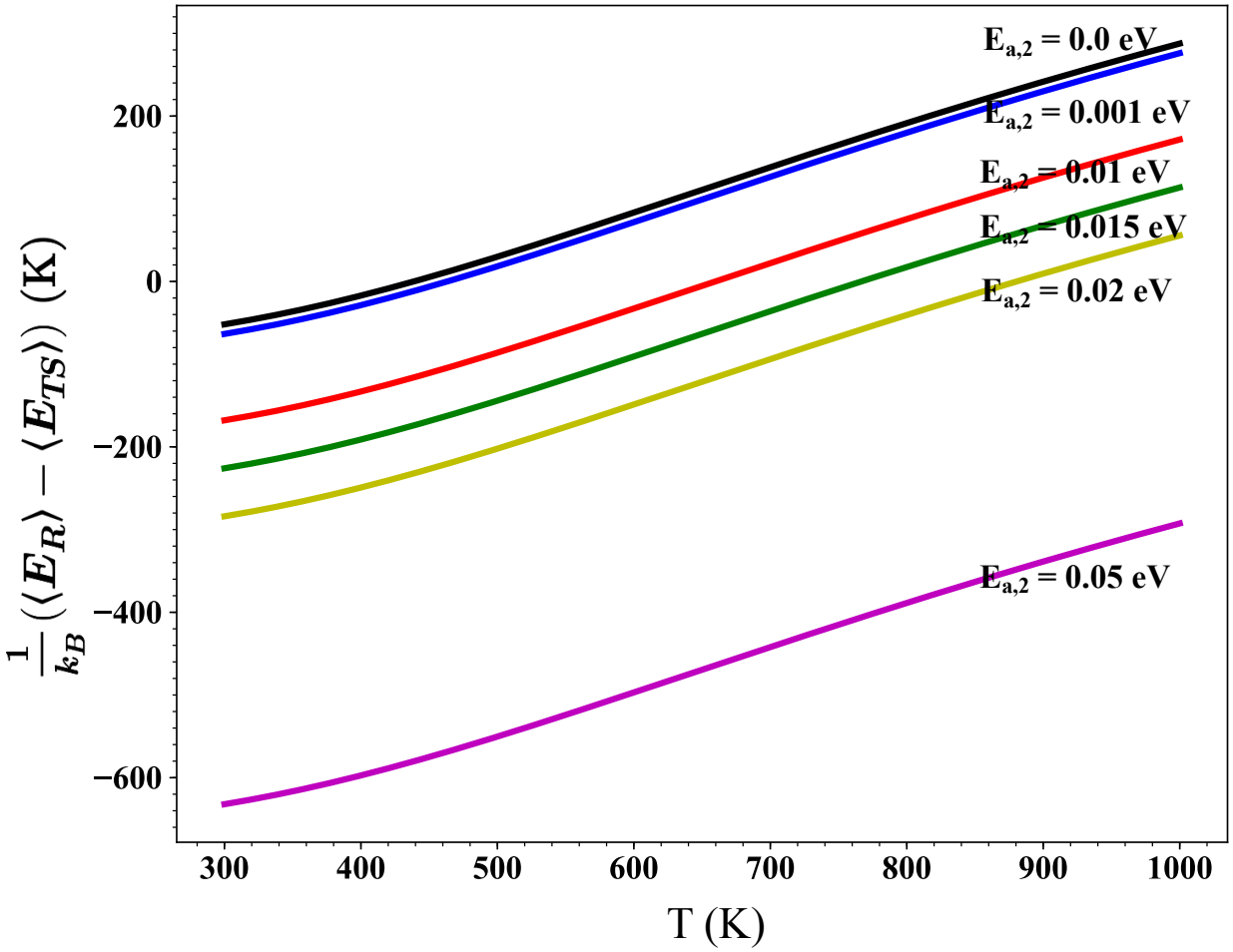

Figure 3. Slope of the ln(k_{ens}) vs. 1/T line as a function of temperature for the ensemble of 5 isomers shown in Figure 2. The temperatures at which the slope becomes zero for $E_{a,2}$ = 0, 0.001, 0.01, 0.15, 0.02, and 0.05 eV are 439, 463, 660, 767, 880 and 2094 K respectively.

In practice, several systems have been found in which the global minimum structure of the catalyst is not the one responsible for the kinetics of the reaction, i.e., a metastable structure with higher energy than the global minimum is found to have lower reaction barrier than that of the global minimum.[11,26] As an example, we look at the ethane dehydrogenation reaction catalyzed by Pt_4/SiO_2 and Pt_4Sn_3/SiO_2.[23] Figure 4 shows the barriers for each thermally-accessible isomer of Pt_4/SiO_2 and Pt_4Sn_3/SiO_2 as well as the Arrhenius plot (ln(k_{ens}) vs. 1/T) obtained for Pt_4/SiO_2 and

Pt_4Sn_3/SiO_2. It is clear that both plots show a highly linear behavior even in the case of Pt_4Sn_3/SiO_2 where the second local minimum structure has the highest rate constant. Comparing to theory, we can attribute this result to the relatively high barriers of the clusters compared to the theoretical investigations, which showed that at least one isomer should have a barrier less than 0.02 eV. In fact, this is one of the main reasons that in practice we do not see non-Arrhenius behavior for the ensemble of fluxional clusters due solely to their dynamicity. It is obvious that other factors such as change in the mechanism of the reaction due to the presence of a metastable isomer, or change of catalyst composition due to a particular reactivity of some of its states, can result in deviating from the Arrhenius behavior; however, such cases are not the focus of this study.

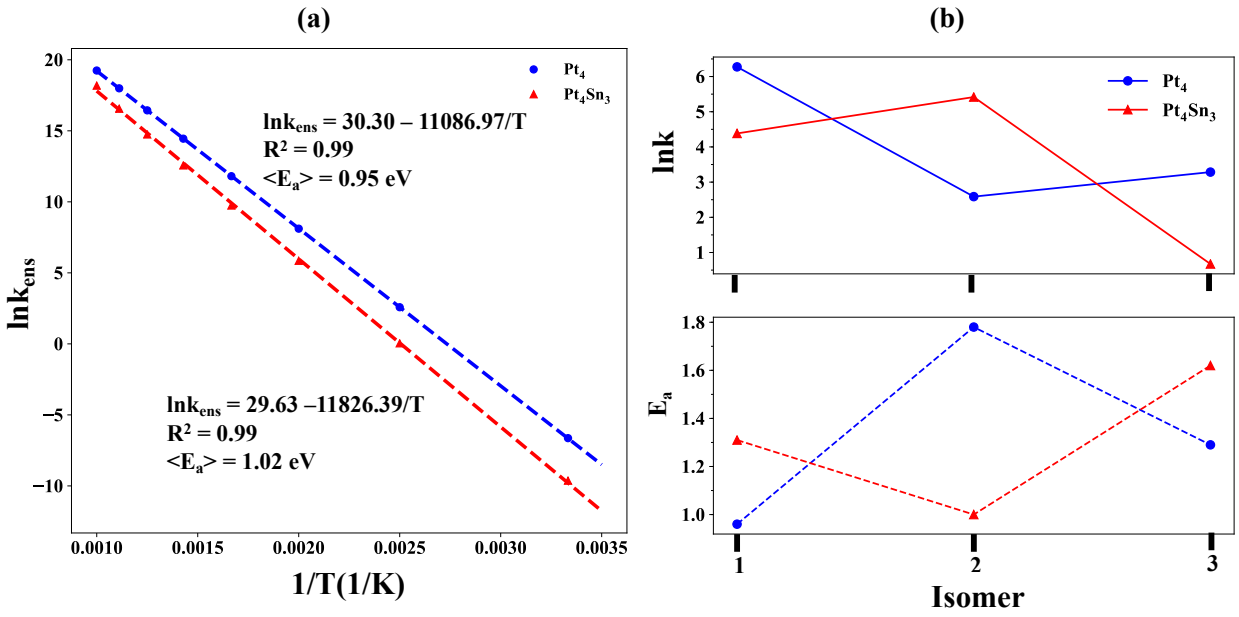

Figure 4. (a) Arrhenius plot of ethylene dehydrogenation reaction catalyzed by Pt_4/SiO_2 and Pt_4Sn_3/SiO_2 in the temperature range of 300 – 1000 K. (b) Rate constants and barriers calculated for each of the 3 isomers of Pt_4/SiO_2 and Pt_4Sn_3/SiO_2 populated at reaction temperature (700 K).

We should also note that, as can be seen from equation (4), both the thermodynamic (change in the Boltzmann population distribution as a function of temperature) and kinetic (different activation energies for different isomers) contributions to the observed rate will play roles in the ensemble not showing a non-Arrhenius behavior. The ensemble approach can lead to a different view of reaction kinetics in addition to thermodynamics. Chemically distinct states of the catalyst

get populated as T increases, and, if these states have barriers significantly different from that of the global minimum, the Arrhenius plot should be nonlinear.

3. Conclusions

In summary, we propose a simple modification to the Arrhenius equation using an ensemble-average representation is to write the ensemble rate constant in terms of rate constant of every state weighted by Boltzmann populations. Moreover, non-Arrhenius behavior can be found in an ensemble of cluster catalysts when at least one of the local minima has a barrier significantly lower (< 0.02 eV) than other local minima. Note that the number of isomers which are energetically close to, or even degenerate with, the global minimum is another key factor for the ensemble to have a nonlinear Arrhenius plot. On the other hand, due to the significantly small barrier requirement, which is in the order of magnitude of kT at room temperature, such a system might not be easily found in practice.

Appendix A

Ensemble average rate constant is defined as

$$k_{ens} = \sum_{i}^{n} P_i A_i e^{\frac{-E_{a,i}}{k_B T}} \tag{A.1}$$

Which can be expanded as

$$k_{ens} = \frac{\sum_i^n e^{\frac{-E_i}{k_B T}} A_i e^{\frac{-E_{a,i}}{k_B T}}}{\sum_i^n e^{\frac{-E_i}{k_B T}}} = \frac{\sum_i^n A_i e^{\frac{-(E_i + E_{a,i})}{k_B T}}}{\sum_i^n e^{\frac{-E_i}{k_B T}}} \tag{A.2}$$

By taking the derivate and assuming that A_i is temperature independent we arrive at

$$\frac{d(lnk_{ens})}{d\left(\frac{1}{T}\right)} = \frac{-T^2}{k_{ens}}\frac{dk_{ens}}{dT}$$

$$= \frac{-T^2}{k_{ens}}\left(\frac{\sum_i^n \frac{(E_i + E_{a,i})}{k_B T^2} A_i e^{\frac{-(E_i+E_{a,i})}{k_B T}} \sum_i^n e^{\frac{-E_i}{k_B T}}}{(\sum_i^n e^{\frac{-E_i}{k_B T}})^2}\right. \tag{A.3}$$

$$\left. - \frac{\sum_i^n A_i e^{\frac{-(E_i+E_{a,i})}{k_B T}} \sum_i^n \frac{E_i}{k_B T^2} e^{\frac{-E_i}{k_B T}}}{(\sum_i^n e^{\frac{-E_i}{k_B T}})^2}\right)$$

Equation (A.3) can be further simplified as

$$\frac{d(lnk_{ens})}{d\left(\frac{1}{T}\right)} = \frac{-1}{k_B k_{ens}}\left(\frac{\sum_i^n (E_i + E_{a,i}) A_i e^{\frac{-(E_i+E_{a,i})}{k_B T}}}{\sum_i^n e^{\frac{-E_i}{k_B T}}} - \frac{\sum_i^n A_i e^{\frac{-(E_i+E_{a,i})}{k_B T}} \sum_i^n E_i e^{\frac{-E_i}{k_B T}}}{(\sum_i^n e^{\frac{-E_i}{k_B T}})^2}\right) \tag{A.4}$$

Substituting k_{ens} into equation (A.4) we get

$$\frac{d(lnk_{ens})}{d\left(\frac{1}{T}\right)} = \frac{-1}{k_B}\frac{\sum_i^n e^{\frac{-E_i}{k_B T}}}{\sum_i^n A_i e^{\frac{-(E_i+E_{a,i})}{k_B T}}}\left(\frac{\sum_i^n (E_i + E_{a,i}) A_i e^{\frac{-(E_i+E_{a,i})}{k_B T}}}{\sum_i^n e^{\frac{-E_i}{k_B T}}}\right. \tag{A.5}$$

$$\left. - \frac{\sum_i^n A_i e^{\frac{-(E_i+E_{a,i})}{k_B T}} \sum_i^n E_i e^{\frac{-E_i}{k_B T}}}{(\sum_i^n e^{\frac{-E_i}{k_B T}})^2}\right)$$

Which can be simplified as

$$\frac{d(lnk_{ens})}{d\left(\frac{1}{T}\right)} = \frac{-1}{k_B}\left(\frac{\sum_i^n (E_i + E_{a,i}) A_i e^{\frac{-(E_i+E_{a,i})}{k_B T}}}{\sum_i^n A_i e^{\frac{-(E_i+E_{a,i})}{k_B T}}} - \frac{\sum_i^n E_i e^{\frac{-E_i}{k_B T}}}{\sum_i^n e^{\frac{-E_i}{k_B T}}}\right) \tag{A.6}$$

By assuming A_i is almost the same for the isomers in the ensemble we arrive at our final formula:

$$\frac{d(lnk_{ens})}{d\left(\frac{1}{T}\right)} = \frac{-1}{k_B}(\langle E_{TS}\rangle - \langle E_R\rangle) = \frac{-\langle E_a\rangle}{k_B} \tag{A.7}$$

Note that we can still include the influence of the pre-exponential factor by using equation (A.6) instead of (A.7) if we are concerned about the difference between the pre-exponential factor of different isomers in the ensemble.

ASSOCIATED CONTENT

Plot which shows the $E_{a,i}$ search space obtained from 40,000 different combinations of $E_{a,1}$ and $E_{a,2}$ in the range of 0 – 2 eV for the ensemble of two isomers with different relative energies E_1 = 0 and E_2 = 0.10, 0.15, 0.20, 0.25, 0.40, and 0.50 eV.

AUTHOR INFORMATION

ORCIDs

Anastassia Alexandrova: 0000-0002-3003-1911

Borna Zandkarimi: 0000-0002-7633-132X

Notes

The authors declare no competing financial interest.

Actual R^2 values and all case study parameters of ensemble of 2 and 5 isomers along with the python code can be found here: https://github.com/bzkarimi/non-Arrhenius

ACKNOWLEDGEMENT

This work was supported by the Air Force Office of Scientific Research under a Basic Research Initiative grant (AFOSR FA9550-16-1-0141). CPU resources at the UCLA–IDRE cluster were used to conduct this work.

REFERENCES

(1) Arrhenius, S. Über Die Reaktionsgeschwindigkeit Bei Der Inversion von Rohrzucker Durch Saüren. *Z. Phys. Chem.* **1889**, *4*, 226–248.

(2) Menzinger, M.; Wolfgang, R. The Meaning and Use of the Arrhenius Activation Energy. *Angew. Chemie Int. Ed. English* **1969**, *8*, 438–444.

(3) Logan, S. R. The Origin and Status of the Arrhenius Equation. *J. Chem. Educ.* **1982**, *59*, 279–281.

(4) Laidler, K. L. The Development of the Arrhenius Equation. *J. Chem. Educ.* **1984**, *61*, 494–495.

(5) Zhang, Z.; Zandkarimi, B.; Alexandrova, A. N. Ensembles of Metastable States Govern Heterogeneous Catalysis on Dynamic Interfaces. *Acc. Chem. Res.* **2020**, *53*, 447–458.

(6) Zhai, H.; Alexandrova, A. N. Fluxionality of Catalytic Clusters: When It Matters and How to Address It. *ACS Catal.* **2017**, *7*, 1905–1911.

(7) Jimenez-Izal, E.; Alexandrova, A. N. Computational Design of Clusters for Catalysis. *Annu. Rev. Phys. Chem.* **2018**, *69*, 377–400.

(8) Zhai, H.; Alexandrova, A. N. Ensemble-Average Representation of Pt Clusters in Conditions of Catalysis Accessed through GPU Accelerated Deep Neural Network Fitting Global Optimization. *J. Chem. Theory Comput.* **2016**, *12*, 6213–6226.

(9) Baxter, E. T.; Ha, M. A.; Cass, A. C.; Alexandrova, A. N.; Anderson, S. L. Ethylene Dehydrogenation on Pt4,7,8 Clusters on Al2O3: Strong Cluster Size Dependence Linked to Preferred Catalyst Morphologies. *ACS Catal.* **2017**, *7*, 3322–3335.

(10) Zhai, H.; Alexandrova, A. N. Local Fluxionality of Surface-Deposited Cluster Catalysts: The Case of Pt7on Al2O3. *J. Phys. Chem. Lett.* **2018**, *9*, 1696–1702.

(11) Sun, G.; Sautet, P. Metastable Structures in Cluster Catalysis from First-Principles: Structural Ensemble in Reaction Conditions and Metastability Triggered Reactivity. *J. Am. Chem. Soc.* **2018**, *140*, 2812–2820.

(12) Zandkarimi, B.; Alexandrova, A. N. Surface-supported Cluster Catalysis: Ensembles of Metastable States Run the Show. *Wiley Interdiscip. Rev. Comput. Mol. Sci.* **2019**, No. April, (April), e1420.

(13) Tolman, R. C. Statistical Mechanics Applied to Chemical Kinetics. *J. Am. Chem. Soc.* **1920**, *42*, 2506–2528.

(14) Truhlar, D. G. Interpretation of the Activation Energy. *J. Chem. Educ.* **1978**, *54*, 309–311.

(15) Piskulich, Z. A.; Mesele, O. O.; Thompson, W. H. Activation Energies and Beyond. *J. Phys. Chem. A* **2019**, *123*, 7185–7194.

(16) Wu, C.; Schmidt, D. J.; Wolverton, C.; Schneider, W. F. Accurate Coverage-Dependence Incorporated into First-Principles Kinetic Models: Catalytic NO Oxidation on Pt (1 1 1). *J. Catal.* **2012**, *286*, 88–94.

(17) Fung, V.; Jiang, D. E. Exploring Structural Diversity and Fluxionality of Ptn (n = 10-13) Clusters from First-Principles. *J. Phys. Chem. C* **2017**, *121*, 10796–10802.

(18) Ha, M. A.; Baxter, E. T.; Cass, A. C.; Anderson, S. L.; Alexandrova, A. N. Boron Switch for Selectivity of Catalytic Dehydrogenation on Size-Selected Pt Clusters on Al2O3. *J. Am. Chem. Soc.* **2017**, *139*, 11568–11575.

(19) Mader, E. A.; Larsen, A. S.; Mayer, J. M. Hydrogen Atom Transfer from Iron(II)-Tris[2,2′- Bi(Tetrahydropyrimidine)] to TEMPO: A Negative Enthalpy of Activation Predicted by the Marcus Equation. *J. Am. Chem. Soc.* **2004**, *126*, 8066–8067.

(20) Bím, D.; Maldonado-Domínguez, M.; Fučík, R.; Srnec, M. Dissecting the Temperature Dependence of Electron-Proton Transfer Reactivity. *J. Phys. Chem. C* **2019**, *123*, 21422–21428.

(21) Parada, G. A.; Goldsmith, Z. K.; Kolmar, S.; Rimgard, B. P.; Mercado, B. Q.; Hammarström, L.; Hammes-schiffer, S.; Mayer, J. M. Concerted Proton-Electron Transfer Reactions in the Marcus Inverted Region. *Science (80-.).* **2019**, *475*, 471–475.

(22) Grampp, G. The Marcus Inverted Region from Theory to Experiment. *Angew. Chemie Int. Ed. English* **1993**, *32*, 691–693.

(23) Suppan, P. The Marcus Inverted Region. *Top. Curr. Chem.* **1992**, *163*, 95–130.

(24) Miller, J. R. Intramolecular Long-Distance Electron Transfer in Radical Anions. The Effects of Free Energy and Solvent on the Reaction Rates1. *J. Am. Chem. Soc.* **1984**, *106*, 3047–3049.

(25) Marcus, R. A. On the Theory of Chemiluminescent Electron-Transfer Reactions. *J. Chem. Phys.* **1965**, *43*, 2654–2657.

(26) Gorey, T.; Zandkarimi, B.; Li, G.; Baxter, E.; Alexandrova, Anastassia; Anderson, S. Coking-Resistant Sub-Nano Dehydrogenation Catalysts: PtnSnx/SiO2 (n = 4, 7). *ACS Catal.* **2020**, *10*, 4543–4558.

TOC Graphic